Linear Generalised Model Predictive Control to Avoid Input Saturation through Matrix Conditions

Mercorelli, Paolo

Published in:
WSEAS Transactions on Systems

Publication date:
2017

Document Version
Publisher's PDF, also known as Version of record

Linear Generalised Model Predictive Control to Avoid Input Saturation through Matrix Conditions

PAOLO MERCORELLI
Institute of Product and Process Innovation
Leuphana University of Lueneburg University
Volgershall 1, D-21339 Lueneburg
GERMANY
mercorelli@uni.leuphana.de

Abstract: The goal of this contribution is presenting a Theorem which states the stability of a feedback controlled system with a Linear Generalized Model Predictive Control (LGMPC). Concerning the stability, a sufficient and constructive condition on the weight matrices of the cost function used in the optimization problem in LGMPC for one step prediction horizon is demonstrated. The condition consists of a lower bound for one of these matrices. The obtained condition is explained and discussed by means of some physical considerations. The second part of this contribution is devoted to the saturation case and proves a sufficient condition for obtaining stability and saturation avoidance. Two case studies are shown using computer simulations at the end of the paper.

Key-Words: - Model predictive control· Optimization· Matrix algebra· Discrete systems· Linear systems ·Applications

1 Introduction

Improvements of the tracking of a desired trajectory are very often achieved by means of a Model predictive control approach. The linear prediction algorithm is used for improvement of the tracking performances of an adaptive controller. Because of that, MPC is commonly used in drives control applications [1, 2]. Constraints and multi-variable industrial processes can be successfully managed by MPC, that is why this control approach has been applied in a wide range of automotive and process control communities [3]. In the meantime, the MPC applications are usually limited by slow dynamic systems because of the computation burden in solving optimization problems on-line [3]. Studying of application of MPC in mechatronic systems for servo design has attracted interest of a great number of researchers. The reason for that is development of a microprocessor technology. There are some advantageous examples in many mechatronic systems such as electrical motor control [4], tow stage actuation system control and machine tool chattering control [5]. There is also a fast development of different advanced techniques integrated within MPC for the performance improvement [6]. One of the most interesting problems in the contest of optimization consists of finding conditions on the stability. In this contribution, lower bounds of matrix which characterizes the cost function are found to guarantee the stability of the optimal solution for one step prediction horizon. The condition is a constructive one and straightforward to be interpreted. This contribution is divided into the following parts. Section 2 proves a property of the LGMPC in case without and with saturation for one step prediction horizon. Section 3 is devoted to present two examples. Conclusions close the paper.

2 A stability sufficient constructive condition in GMPC

Theorem 1 Let us take the discrete SISO linear system into consideration:

$$\mathbf{z}(\mathrm{k}+1) = \mathbf{A}_{\mathrm{k}}\mathbf{z}(\mathrm{k}) + \mathbf{B}_k u_{mpc}(k), \qquad (1)$$

$$\mathrm{y}(\mathrm{k}) = \mathbf{H}_{\mathrm{k}}\mathbf{z}(\mathrm{k}), \qquad (2)$$

which is obtained by a discretization of linear continuous system a sampling time which equals T_s. $u_{mpc}(k)$ represents the first element of the vector of the optimal solution as calculated in [7] for the following cost function:

$$J = \frac{1}{2}\sum_{j=1}^{N}\left(y_d(k+j) - \hat{y}(k+j)\right)^T \mathbf{Q}_p\left(y_d(k+j) - \hat{y}(k+j)\right) + \sum_{j=1}^{N}\left(\Delta u_{mpc}(k+j-1)\right)^T \boldsymbol{R}_p \Delta u_{mpc}(k+j-1), \quad (3)$$

where $u_{mpc}(k) = u_{mpc}(k) - u_{mpc}(k-1)$, $y_d(k+j)$, $j = 1,2,\dots,N$ *is the* output reference trajectory and N is the prediction horizon, and $\mathbf{Q}_p$ and $\mathbf{R}_p$ are non-negative definite matrices. Furthermore, the solution minimizing performance index (3) may be obtained by solving:

$$\frac{\partial J}{\partial \Delta \mathbf{U}_{mpc}} = 0. \quad (4)$$

It is known for instance from [7] that the optimal solution is:

$$\Delta u_{mpc}(k) = (\mathbf{F}_{1p}^T \mathbf{Q}_p \mathbf{F}_{1p} + \mathbf{R}_p)^{-1} \mathbf{F}_{1p}^T \mathbf{Q}_p \left(\mathbf{Y}_{d_p}(k) - \mathbf{G}_p \mathbf{z}(k)\right), \quad (5)$$

In which in case of one step prediction horizon $\mathbf{F}_{1_p} = \mathbf{H}_k \mathbf{B}_k$ and $\mathbf{G}_p = \mathbf{H}_k \mathbf{A}_k$ and where $\mathbf{Y}_{d_p}(k)$ is the desired output column vector. Matrices $\mathbf{Q}_p$ and $\mathbf{R}_p$ are diagonal and positive defined. Under the hypothesis that system (5) is asymptotically stable, i.e. $(\|\mathbf{A}_k\|_2 < 1)$, where

$$\|\mathbf{A}_k\|_2 = \sqrt{max\lambda_i(\mathbf{A}_k^T \mathbf{A}_k)} \text{ for i=1,2,…, n} \in \text{N}$$

represents the root of the maximal eigenvalue of matrix $\mathbf{A}_k^T \mathbf{A}_k, then \; \forall \; \mathbf{R}_p$ diagonal and positive defined matrix such that:

$$\|\mathbf{R}_p\|_2 > \frac{\|\mathbf{B}_k \mathbf{F}_{1p}^T \mathbf{Q}_p \mathbf{G}_p\|_2}{1 - \|A_k\|_2} \quad (6)$$

and

$$\|\mathbf{A}_k - \mathbf{B}_k (\mathbf{F}_{1p}^T \mathbf{Q}_p \mathbf{F}_{1p} + \mathbf{R}_p)^{-1} \mathbf{F}_{1p}^T \mathbf{Q}_p \mathbf{G}_p\|_2 < \|\mathbf{A}_k + \mathbf{B}_k (\mathbf{F}_{1p}^T \mathbf{Q}_p \mathbf{F}_{1p} + \mathbf{R}_p)^{-1} \mathbf{F}_{1p}^T \mathbf{Q}_p \mathbf{G}_p\|_2, \quad (7)$$

The system (1) results to be asymptotically stable for one step prediction horizon. It is to notice that matrix $\mathbf{R}_p$ collapses in a scalar in case of one step prediction horizon, $\mathbf{R}_p$ =r.

Combining Eq. (1) with (5), this expression is obtained:

Proof 1 For one prediction step is considered, then according to [7], it follows that:

$$\mathbf{F}_{1_p} = [\mathbf{H}_k \mathbf{B}_k], \quad (8)$$

$$\mathbf{G}_p = [\mathbf{H}_k \mathbf{A}_k]. \quad (9)$$

Combining Eq. (1) with (5), this expression is obtained:

$$\mathbf{z}(k+1) = \mathbf{A}_k \mathbf{z}(k) + \mathbf{B}_k (\mathbf{F}_{1p}^T \mathbf{Q}_p \mathbf{F}_{1p} + \mathbf{R}_p)^{-1} \mathbf{F}_{1p}^T \mathbf{Q}_p \left(\mathbf{Y}_{d_p}(k) - \mathbf{G}_p \mathbf{z}(k)\right), \quad (10)$$

which is equivalent to write:

$$\mathbf{z}(k+1) = \left(\mathbf{A}_k - \mathbf{B}_k (\mathbf{F}_{1p}^T \mathbf{Q}_p \mathbf{F}_{1p} + \mathbf{R}_p)^{-1} \mathbf{F}_{1p}^T \mathbf{Q}_p \mathbf{G}_p\right) \mathbf{z}(k) + \mathbf{B}_k (\mathbf{F}_{1p}^T \mathbf{Q}_p \mathbf{F}_{1p} + \mathbf{R}_p)^{-1} \mathbf{F}_{1p}^T \mathbf{Q}_p \mathbf{Y}_{d_p}(k). \quad (11)$$

If

$$\|\mathbf{R}_p\|_2 > \frac{\|\mathbf{B}_k \mathbf{F}_{1p}^T \mathbf{Q}_p \mathbf{G}_p\|_2}{1 - \|A_k\|_2},$$

considering that $\|\mathbf{R}_p\| > 0$,

$$\|\mathbf{A}_k\|_2 + \|\mathbf{R}_p\|_2^{-1} \|\mathbf{B}_k \mathbf{F}_{1p}^T \mathbf{Q}_p \mathbf{G}_p\|_2 < 1. \quad (13)$$

Considering that $\|\mathbf{R}_p\|_2 = r$ is a scalar, the following condition can be derived:

$$\|\mathbf{A}_k\|_2 + \|\mathbf{B}_k r^{-1} \mathbf{F}_{1p}^T \mathbf{Q}_p \mathbf{G}_p\|_2 < 1. \quad (14)$$

Being expression $\mathbf{F}_{1p}^T \mathbf{Q}_p \mathbf{F}_{\mathbf{1}p}$ a scalar for one step prediction horizon and

$$\mathbf{F}_{1p}^T \mathbf{Q}_p \mathbf{F}_{\mathbf{1}p} > 0,$$

as a consequence, it follows that:

$$\|\mathbf{A}_k\|_2 + \|\mathbf{B}_k (\mathbf{F}_{1p}^T \mathbf{Q}_p \mathbf{F}_{1p} + r)^{-1} \mathbf{F}_{1p}^T \mathbf{Q}_p \mathbf{G}_p\|_2 < 1. \quad (15)$$

Considering the norm properties and condition (7), then:

$$\begin{aligned}&\|\mathbf{A}_k - \mathbf{B}_k(\mathbf{F}_{1p}^T\mathbf{Q}_p\mathbf{F}_{1p}+\mathrm{r})^{-1}\mathbf{F}_{1p}^T\mathbf{Q}_p\mathbf{G}_p\|_2\\ &< \|\mathbf{A}_k + \mathbf{B}_k(\mathbf{F}_{1p}^T\mathbf{Q}_p\mathbf{F}_{1p}+\mathrm{r})^{-1}\mathbf{F}_{1p}^T\mathbf{Q}_p\mathbf{G}_p\|_2\\ &< \|\mathbf{A}_k\|_2 + \|\mathbf{B}_k(\mathbf{F}_{1p}^T\mathbf{Q}_p\mathbf{F}_{1p}+\mathrm{r})^{-1}\mathbf{F}_{1p}^T\mathbf{Q}_p\mathbf{G}_p\|_2\\ &< 1\end{aligned} \quad (16)$$

To conclude:

$$\|\mathbf{A}_k - \mathbf{B}_k(\mathbf{F}_{1p}^T\mathbf{Q}_p\mathbf{F}_{1p}+\mathrm{r})^{-1}\mathbf{F}_{1p}^T\mathbf{Q}_p\mathbf{G}_p\|_2 < 1. \quad (17)$$

Condition (1) states that the eigenvalues of the controlled system described by (11) are all inside the complex unit circle and thus system (11) results to be asymptotically stable.
Stability represents the necessary condition of the optimality of a controlled system. In order to interpret the result, let us observe a linear mechanical system including a mass-spring system in which it is known that the eigenvalues can variate in the whole real and complex domain as functions of the mass which state the system dynamics. The following considerations can be done:

- Case of high inertial system:
  This is the case in which mass $m\to+\infty$, then, because of the discretisation, it follows:
  $(\|\mathbf{A}_k\|_2 - 1\|) \to 0$, with, according to the Landau notation, $\mathcal{O}(\|\mathbf{A}_k\|_2 - 1) = \mathcal{O}\left(\frac{1}{m}\right)$, but in the meantime, $\mathcal{O}\left(\mathbf{B}_k\mathbf{F}_{1p}^T\right) = \mathcal{O}\left(\mathbf{B}_k\mathbf{B}_k^T\right) = \mathcal{O}\left(\frac{1}{m^2}\right)$. For a very slow system, $\|\mathbf{R}_p\|_2 \to 0$ and parameter $\|\mathbf{R}_p\|_2$, according to (6), is present in the denominator function of the optimal solution of (5) and in this case, small values are devoted to speed up the system.
- Case of low inertial system:
  This is the case in which mass $m\to 0$, then, because of the discretisation, it follows:
  $\|\mathbf{A}_k\|_2 \to 0$, with $\mathcal{O}(\|\mathbf{A}_k\|_2) = \mathcal{O}\left(\frac{1}{m}\right)$, but in the meantime, $\mathcal{O}\left(\mathbf{B}_k\mathbf{F}_{1p}^T\right) = \mathcal{O}\left(\mathbf{B}_k\mathbf{B}_k^T\right) \to +\infty$ in which $\mathcal{O}\left(\mathbf{B}_k\mathbf{B}_k^T\right) = \mathcal{O}\left(\frac{1}{m^2}\right)$. For a very fast system $\|\mathbf{R}_k\|_2 \to +\infty$ and $\mathbf{R}_p$, according to (6), is present in the denominator function of the optimal solution in (5) and in this case, large values are devoted to slow down the system.

So, it is possible to conclude that a high inertial system needs relatively small values of $\|\mathbf{R}_p\|_2$ to be stabilised. On the contrary, a low inertial system needs large values of $\|\mathbf{R}_p\|_2$ to be stabilised.

2.1 The saturation case

Proposition 1 Let us take the following discrete SISO linear system as before into consideration:

$$\mathbf{z}(\mathrm{k}+1) = \mathbf{A}_\mathrm{k}\mathbf{z}(\mathrm{k}) + \mathbf{B}_k u_{mpc}(\mathrm{k}), \quad (18)$$

$$\mathrm{y}(\mathrm{k}) = \mathbf{H}_\mathrm{k}\mathbf{z}(\mathrm{k}), \quad (19)$$

and let U_{max} a real value with

$$\left|u_{mpc}(\mathrm{k})\right| < \mathrm{U}_{\max}\ \forall k, \quad (20)$$

Then (18) with the input saturation defined in (20) and controlled with the control law in (5) is asymptotically stable and its input avoids the saturation constraint if the following conditions hold:

$$\mathrm{r} = \|\mathbf{R}_p\|_2 > max\left\{\frac{\|\mathbf{B}_k\mathbf{F}_{1p}^T\mathbf{Q}_p\mathbf{Y}_{\mathbb{d}_p}(k)\|_2}{\mathrm{U}_{max}} - \|\mathbf{F}_{1p}^T\mathbf{Q}_p\mathbf{F}_{1p}\|_2, \frac{\|\mathbf{B}_k\mathbf{F}_{1p}^T\mathbf{Q}_p\mathbf{G}_p\|_2}{1-\|\mathbf{A}_k\|_2}\right\}, \quad (21)$$

and

$$\begin{aligned}&\|\mathbf{A}_k - \mathbf{B}_k(\mathbf{F}_{1p}^T\mathbf{Q}_p\mathbf{F}_{1p}+\mathbf{R}_p)^{-1}\mathbf{F}_{1p}^T\mathbf{Q}_p\mathbf{G}_p\|_2 <\\ &\|\mathbf{A}_k + \mathbf{B}_k(\mathbf{F}_{1p}^T\mathbf{Q}_p\mathbf{F}_{1p}+\mathbf{R}_p)^{-1}\mathbf{F}_{1p}^T\mathbf{Q}_p\mathbf{G}_p\|_2,\end{aligned} \quad (22)$$

Proof 2 The demonstration is straightforward. In fact, just considering that:

$$\left|u_{mpc}(\mathrm{k})\right| < \mathrm{U}_{\max}\ \forall k,$$

and thus, considering the input of the optimal predicted expression (11), it is enough that the following condition holds:

$$\|\mathbf{B}_k(\mathbf{F}_{1p}^T\mathbf{Q}_p\mathbf{F}_{1p}+\mathbf{R}_p)^{-1}\mathbf{F}_{1p}^T\mathbf{Q}_p\mathbf{Y}_{\mathbb{d}_p}(k)\|_2 < \mathrm{U}_{\max}. \quad (23)$$

This can be written as:

$$\begin{aligned}&\|\mathbf{B}_k(\mathbf{F}_{1p}^T\mathbf{Q}_p\mathbf{F}_{1p}+\mathbf{R}_p)^{-1}\mathbf{F}_{1p}^T\mathbf{Q}_p\mathbf{Y}_{\mathbb{d}_p}(k)\|_2 <\\ &\|(\mathbf{F}_{1p}^T\mathbf{Q}_p\mathbf{F}_{1p}+\mathbf{R}_p)^{-1}\|_2\,\|\mathbf{B}_k\mathbf{F}_{1p}^T\mathbf{Q}_p\mathbf{Y}_{\mathbb{d}_p}(k)\|_2 <\\ &\mathrm{U}_{\max}.\end{aligned} \quad (24)$$

Considering that $\mathbf{R}_p$ and $\mathbf{F}_{1p}^T \mathbf{Q}_p \mathbf{F}_{1p}$ are both positiv scalars in case of one step prediction horizon, then:

$$\|\mathbf{F}_{1p}^T \mathbf{Q}_p \mathbf{F}_{1p} \mathbf{R}_p\|_2 < \frac{\|\mathbf{B}_k \mathbf{F}_{1p}^T \mathbf{Q}_p \mathbf{Y}_{\mathbb{d}_p}(k)\|_2}{\mathrm{U}_{max}}. \quad (25)$$

and thus, to guarantee asymptotic stability and anti-saturation input of system (18), it follows:

$$\mathrm{r} = \|\mathbf{R}_p\|_2 > max\left\{\frac{\|\mathbf{B}_k \mathbf{F}_{1p}^T \mathbf{Q}_p \mathbf{Y}_{\mathbb{d}_p}(k)\|_2}{\mathrm{U}_{max}} - \|\mathbf{F}_{1p}^T \mathbf{Q}_p \mathbf{F}_{1p}\|_2, \frac{\|\mathbf{B}_k \mathbf{F}_{1p}^T \mathbf{Q}_p \mathbf{G}_p\|_2}{1-\|\mathbf{A}_k\|_2}\right\}. \quad (26)$$

Remark 1

Concerning saturation phenomena, when saturation happens, the feedback loop is effectively broken. The value at the output of the controller can become very large and often degrades the closed-loop performance in the form of large overshoot, long settling time and sometimes even instability.

3 Simulation examples

3.1 The boiler example

Water regeneration problem is one of the most important issues of some countries. In the last years many efforts were made to propose systems to recycle, regenerate and store cleaned water from waste water. Some of these systems still suffer of lack of automation structure which should guarantee high efficiency and an improvement of the quality of the regenerated water. A great advancement of the control theory together with the development of intelligent control algorithms took place in the research in the last years.

The main nomenclature:

$m_{in}(t)$: input mass flow (kg/sec)
$m_o(t)$: output mass flow (kg/sec)
$m_o(t)$: mass (Kg)
$\frac{dm(t)}{dt}$: mass flow (kg/sec)
$p(t)$: pressure inside of the evaporator
T: Temperature (K)
V: Volume (1)
R_g: vapor constant

Figure 1 demonstrates a schematic representation of the tested system. The following three elements are parts of this system: a boiler, a compressor and an evaporator. The waste water stays in the middle part and the lower part of the boiler. The upper part a vapor chamber is dedicated to keep the water vapor produced after heating the waste water. At first, the waste water is heated by a resistor system until the water vapor appears in the vapor chamber. At this time, the heating is turned off and the compressor is turned on. A high pressure must be obtained in the evaporator by means of the compressor. In the meantime, the compressor should reduce the pressure in the vapor chamber by means of a mass flow. This mass flow ($m_o(t)$) after the condensed phase is purified water in the output of the evaporator. This water is also stilled. The vapor is condensed after giving heat to the waste water in the evaporator. The compressor keeps a low pressure in the vapor chamber to be able to guarantee the new waste water entering from the upper part. The compressor works as a controller in this case. Its output is represented by the mass flow $m_o(t)$ with the constraint that $m_o(t) > 0$. The compressor consists of an asynchronous motor controlled by means of an inverter piloted by a PWM signal. It converts the output of the LMPC controller in frequency. The pressure error occurs in input to LMPC controller. Anyway, the dynamics of the asynchronous motor with the inverter and all other converters are much faster than the one of the controlled process. Short description of the drain: in the initial phase the pressure in the container is the same as the ambient pressure (circa 1.013 bar). After the heating process the pressure increases gradually creases gradually and the evaporating phase of the water starts. When switching of the fan is reduced, the temperature increases in the “internal exchanger”. The water boils and evaporates faster at lower pressure. New water is added by a continuous control with floats. The condensed water vapor from the “internal heat exchanger” is purified. The dynamical model of the system must be taken into account for controller design purposes. Considering that the control process begins after the heating phase and when the water vapor appears in the boiler, the following equations can be taken into consideration.

$$\frac{dm(t)}{dt} = m_i(t) - m_o(t), \quad (27)$$

$$\frac{dp(t)}{dt} = \frac{dm(t)}{dt}\frac{R_g \mathrm{T}}{V}, \quad (28)$$

in which $m_i(t)$ is a stepwise positive constant function. Considering the Forward Euler discretisation with sampling time T_s, the following expression is obtained:

$$m(k+1) = T_s\big(m_i(k) - m_o(k)\big) + m(k), (29)$$

$$p(k+1) = \big(m_i(k) - m_o(k)\big)\frac{R_g \mathrm{T}}{V} + p(k), (30)$$

and thus

$$\begin{bmatrix} m(k+1) \\ p(k+1) \end{bmatrix} = \begin{bmatrix} T_s & 0 \\ 0 & 1 \end{bmatrix} \begin{bmatrix} m(k) \\ p(k) \end{bmatrix} + \begin{bmatrix} T_s \\ \frac{T_{sR_gT}}{V} \end{bmatrix} (m_i(k) - m_0(\mathrm{k})),$$

$$where\ z(k+1) = \begin{bmatrix} m(k+1) \\ p(k+1) \end{bmatrix}, A_k = \begin{bmatrix} T_s & 0 \\ 0 & 1 \end{bmatrix},$$

$$z_k = \begin{bmatrix} m(k) \\ p(k) \end{bmatrix}, B_k = \begin{bmatrix} T_s \\ \frac{T_{sR_gT}}{V} \end{bmatrix},\ u_{mpc(t)=}\ (m_i(k) - m_0(\mathrm{k})). \quad (31)$$

Concerning the simulation results, it should be noted that function $m_i(t)$ is a stepwise constant function with $m_i(t)$=0.086 (kg/sec.) or $m_i(t)$=0 and in the simulated case $m_i(t)$=0.086 (kg/sec.) is considered. As already explained, in the simulations
two cases should be distinguished: weak anti-saturating action:

$$r_{(1,1)} > \frac{\mathbf{B}_k \mathbf{B}_k^T \|\mathbf{Y}_{dp}(k)\|}{\mathrm{U}_{max}}, \quad (32)$$

and strong anti-saturating action:

$$r_{(1,1)} >> \frac{\mathbf{B}_k \mathbf{B}_k^T \|\mathbf{Y}_{dp}(k)\|}{\mathrm{U}_{max}}. \quad (33)$$

The controlled pressure which is the main result of this contribution is demonstrated in the top part of Fig. 2. If the anti-saturating action is weak, it is necessary that the anti-saturating controller has time to re-establish the control loop. During the saturation effect the feedback control is broken, so the long remaining of the pressure at negative values can be explained by the lack of the feedback control action. It is well seen from the low part of Fig. 2 demonstrating the mass flow $\frac{dm(t)}{dt} = m_{in}(t) - m_0(t)$ (kg/sec) that this function is resulting with the relation:

$$\frac{dm(t)}{dt} \approx \frac{dp(t)}{dt}. \quad (34)$$

If we take the following equation one more time into account:

$$\frac{dm(t)}{dt} = m_{in}(t) - m_0(t), \quad (35)$$

a strong initial action through the mass flow $m_0(t)$ is necessary for starting the process. After considering these two figures it becomes visible that the controlled system through the anti-saturating action leaves the saturation very quickly having faster dynamic. This occurs in case of strong anti-saturating action and its effect is represented in the top and low parts of Fig. 3. The faster dynamics are obtained due to the stronger anti-saturating action letting the fast reactivation of the control loop. In presence of saturation the control loop is open and no feedback control occurs.

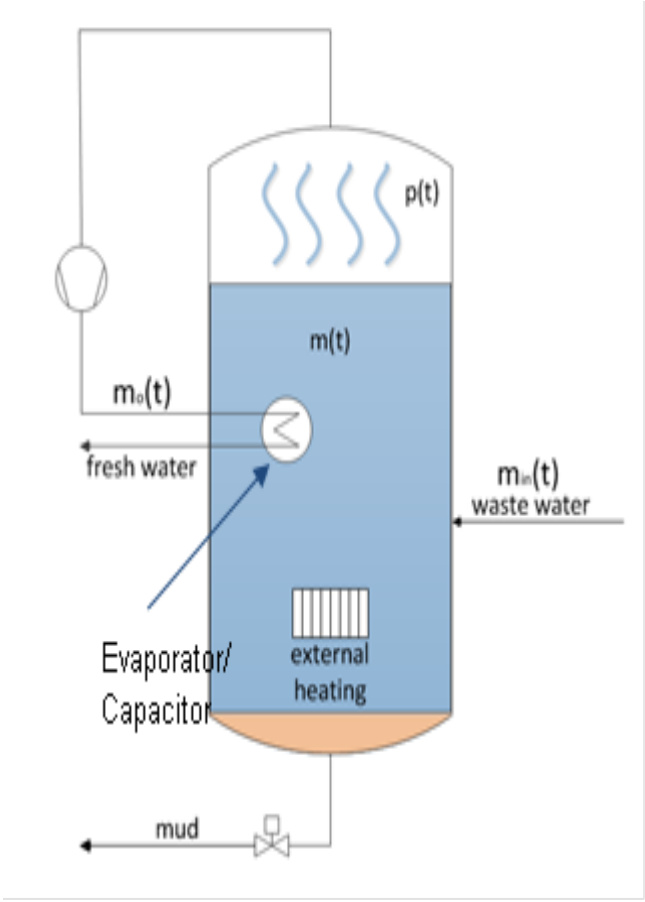

Fig. 1 Boiler system

More in depth, analysing the simulations of Fig. 2 it is possible to remark that in case of weak anti-saturation action, a high input mass flow is generated because of a small value of the elements

of matrix **Q** which allow large value of the input calculated as a result of the optimal solution. Figure 3 indicates the opposite effect, in which large value of matrix **Q** allows a small input mass flow. As a consequence of that, the saturation is avoided and an adequate control is obtained. A wider discussion of this effect is given in the second example.

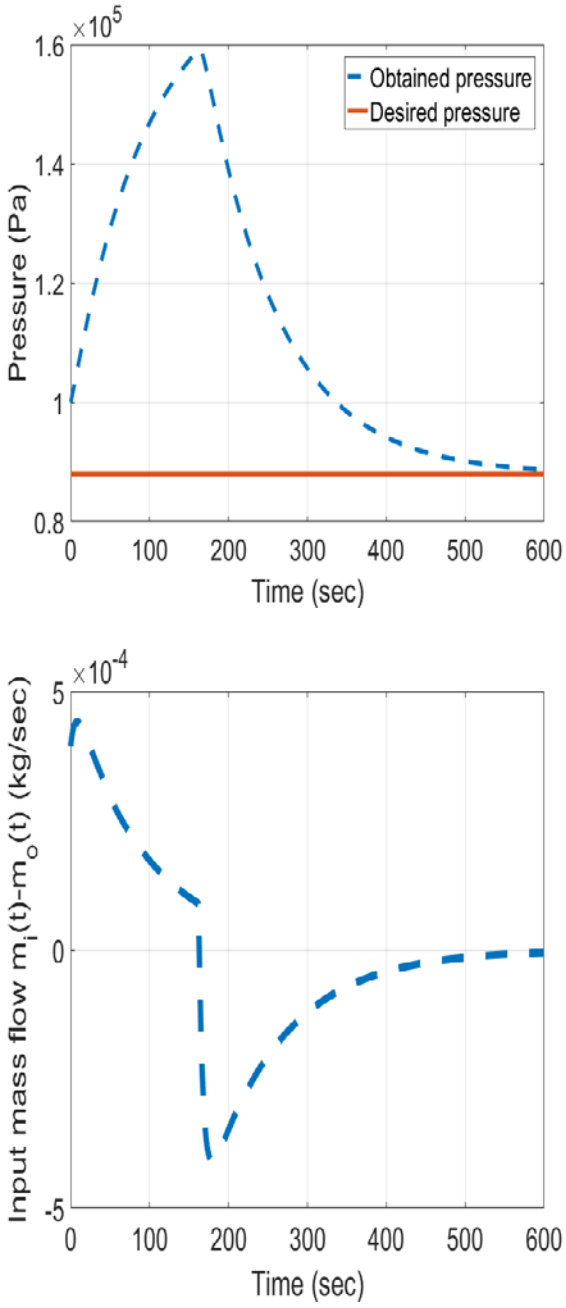

Fig. 2 Top: desired and obtained pressure with week anti-saturating action**. Fig. 2** Low**:** mass flow $\frac{m(t)}{dt} = m_{in}(t) - m_0(t)$ (kg/sec.) with weak anti-saturating action.

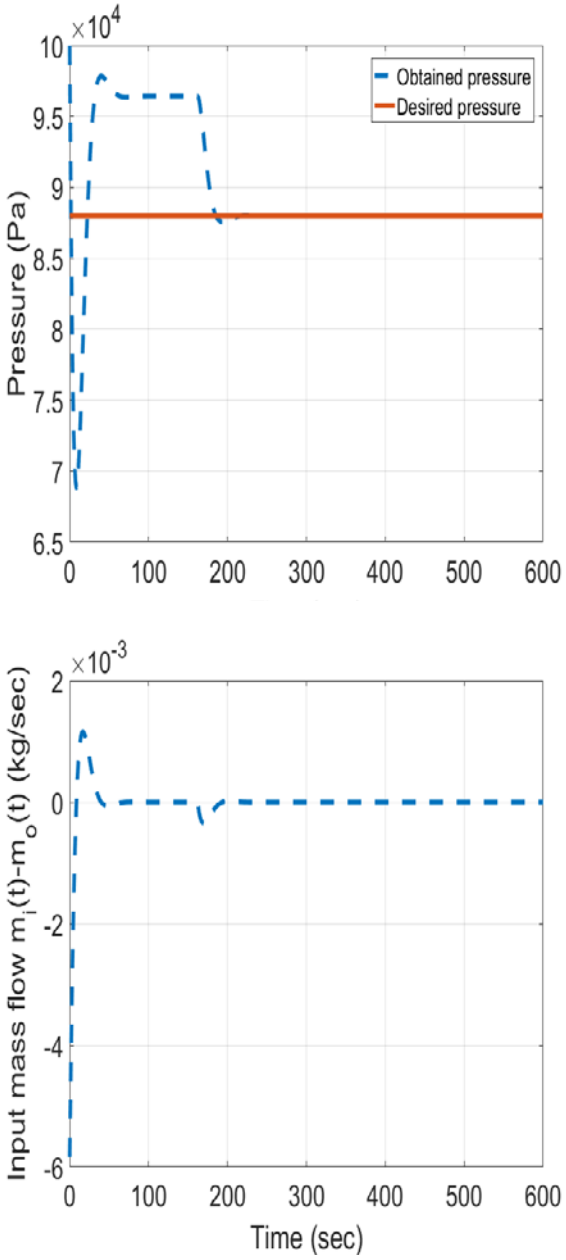

Fig. 3 Top: desired and obtained pressure with strong anti-saturating action. Low: mass flow $\frac{dm(t)}{dt} = m_{in}(t) - m_0(t)$ (kg/sec.) with strong anti-saturating action.

3.2 DC-Drive example

DC drives can be in a significant percentage of a plant load in many industrial facilities. They are commonly used in the plastics, rubber, paper, textile, printing, oil, chemical, metal, and mining industries. These drives are still the most common types of motor speed control for applications requiring very fine control over wide speed ranges with high torques. In Fig. 4, the electrical equivalent circuit of a DC-drive is considered and in Fig. 5 and 6 the schematic structure of the rotor is indicated.

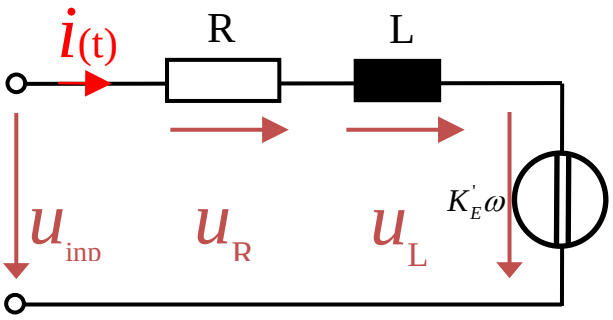

Fig. 4 Electrical equivalent circuit

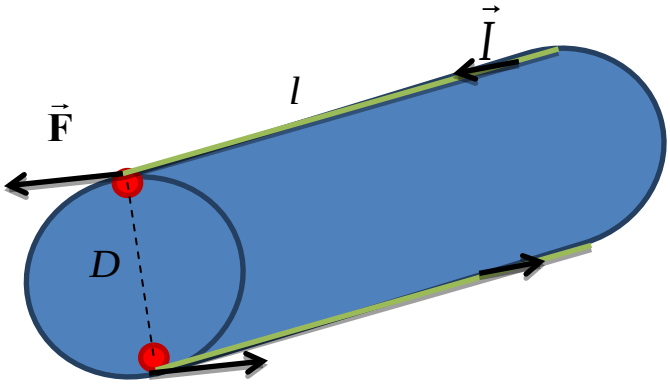

Fig. 5 Rotor of the drive

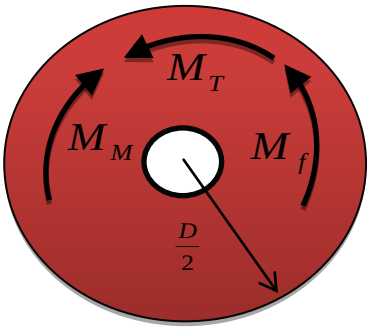

Fig. 6 Section of the rotor of the drive

Considering scheme of Fig. 4 the following linear model of the drive is obtained:

$$\frac{di(t)}{dt} = \frac{1}{L}\left(u_{inp}(t) - Ri(t) - K_E'\omega(t)\right), \quad (36)$$

$$\frac{d\omega(t)}{dt} = \frac{1}{J}\left(K_M' i(t) - K_f'\omega(t)\right), \quad (37)$$

where parameter L represents the inductance, R represents the resistance of the coil of the motor, $K_M' = K_E'$ is the characteristic coefficient of the motor and K_f' the friction constant. After the forward Euler discretization for the current, angular velocity and input voltage, the following expressions are obtained:

$$i(t) = i\big((k-1)T_s\big) = i(k-1) \;\; \forall k = 1,2,\dots n, \quad (38)$$

$$\omega(t) = \omega(k-1), \quad (39)$$

$$u_{inp}(t) = u_{inp}(k-1), \quad (40)$$

and

$$\frac{di(t)}{dt} = \frac{i(k)-i(k-1)}{T_s}, \quad (41)$$

$$\frac{d\omega(t)}{dt} = \frac{\omega(k)-\omega(k-1)}{T_s}. \quad (42)$$

Inserting expression (38), (39), (40), (41) and (42) into (36) and (37), the following expressions are obtained:

$$\frac{i(k)-i(k-1)}{T_s} = \frac{u_{inp}(k-1)}{L} - \frac{K_M' \omega(k-1)}{L} - \frac{Ri(k-1)}{L} \Rightarrow$$
$$i(k) = \left(1 - \frac{RT_s}{L}\right) i(k-1) \frac{K_M' T_s}{L} \omega(k-1) - \frac{u_{inp}(k-1)T_s}{L}, \quad (43)$$

and

$$\frac{\omega(k) - \omega(k-1)}{T_s} = \frac{K_f' \omega(k-1)}{J} \mp \frac{K_M'(k-1)}{J}$$
$$\Rightarrow \omega(k)\left(1 - \frac{K_f' T_s}{J}\right)\omega(k-1) + \frac{K_M' T_s}{J} i(k-1). \quad (44)$$

If (43) and (44) are written in a matrix form, then

$$\begin{bmatrix} i(k) \\ \omega(k) \end{bmatrix} = \begin{bmatrix} 1 - \frac{RT_s}{L} & -\frac{K_M' T_s}{L} \\ \frac{K_M' T_s}{J} & 1 - \frac{K_f' T_s}{J} \end{bmatrix} \begin{bmatrix} i(k-1) \\ \omega(k-1) \end{bmatrix} + \begin{bmatrix} \frac{T_s}{L} \\ 0 \end{bmatrix} u_{inp}(k-1)$$

In Fig. 7 and Fig. 8 the data sheet of the considered motor is reported.

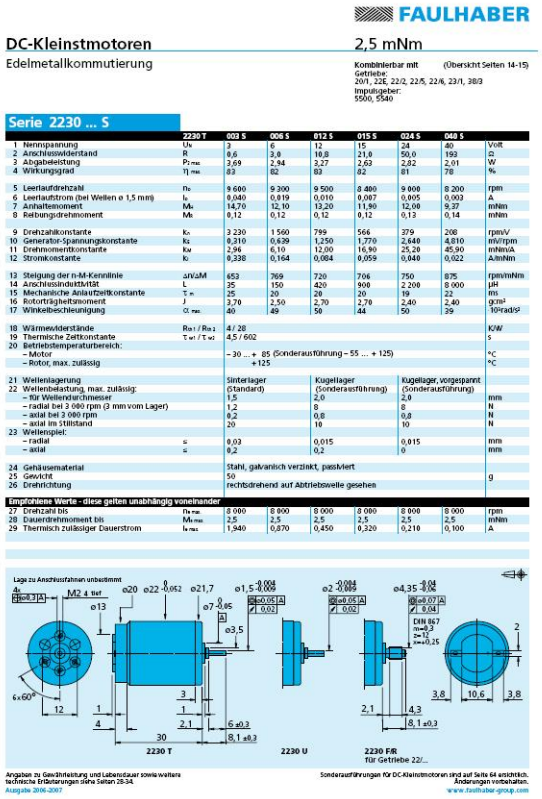

Fig. 7 Data sheet

Description	Notation	Value
Resistance	R	10,8 Ω
Input voltage	U_{in}	12 V
Inductance	L	420 µH
DC-Motor constant	K_E	1,25 mV/rpm (rpm: rounds per minute)
Inertia of the rotor	J	$2{,}7*10^{-7}$ Kg*m^2
DC-Motor constant	K_M	$12*10^{-3}$*Nm/A
Loadless current (nominal current)	I_0	10mA
Loadless number of cycles (nominal cycles)	n_0	9500rpm=158,33rps (rps: rounds per second)
Friction constant	K_R	It must be calculated!

Fig. 8 Data sheet

In Fig. 9 the tracking of the velocity is shown with a strong anti-saturating action. From this figure it is possible to observe a bias due to the limit of the input signal as a consequence of large values of the elements of matrix **Q**. In Fig. 10 the corresponding current in case of a strong anti-saturating action is shown. Figure 11 shows the case in which no anti-saturating action is applied and in Fig. 12 its resulting current is shown. It is possible to see an unstable effect due to the small values of matrix **Q** which induce a large value of the input signal, saturation and a possible instability. Figure 13 shows the case, in which a compromise between non-saturation action but in the meantime non-excessive values of the elements of matrix **Q** are considered. In this situation, the saturation is avoided and in the meantime an enough input voltage is obtained to achieve an adequate tracking. Figure 14 shows the corresponding current of this possible configuration. In general, this technique is a heuristic one and it is based on the barrier

concept of the cost function. The barrier is represented by the input squared term multiplied by the weight matrix **Q**. This barrier represents the power input which together with the squared error tracking states the cost function which represents a compromise between tracking precision and power input to realize this tracking precision.

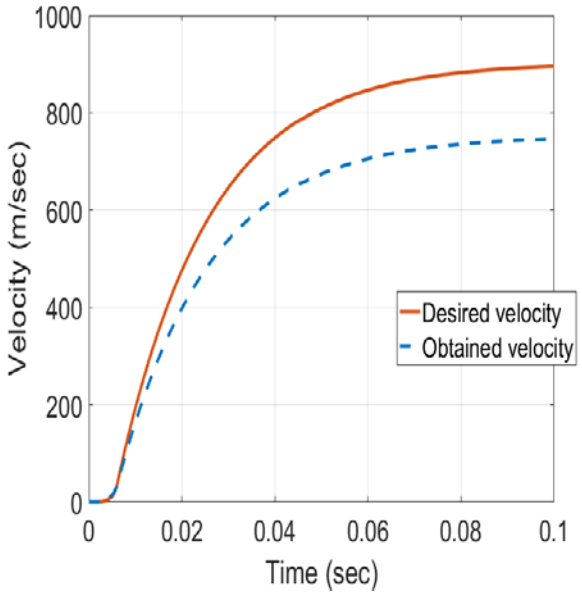

Fig. 9 Velocity tracking with strong anti-saturating action

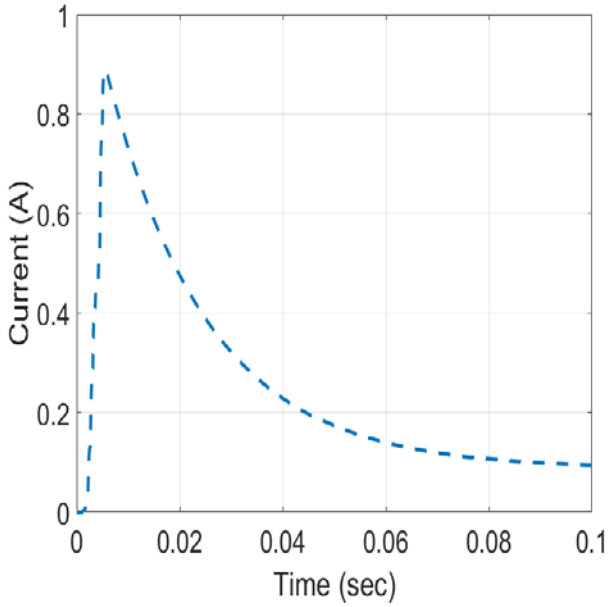

Fig. 10 Current voltage with strong anti-saturating action

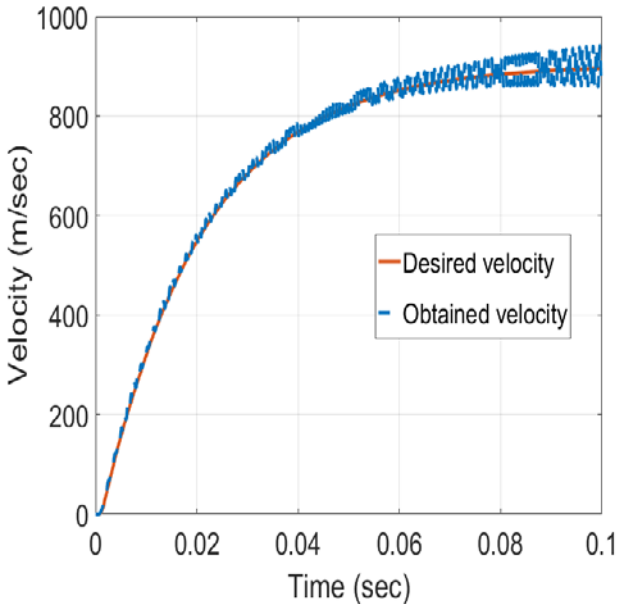

Fig. 11 Velocity tracking with without anti-saturating action

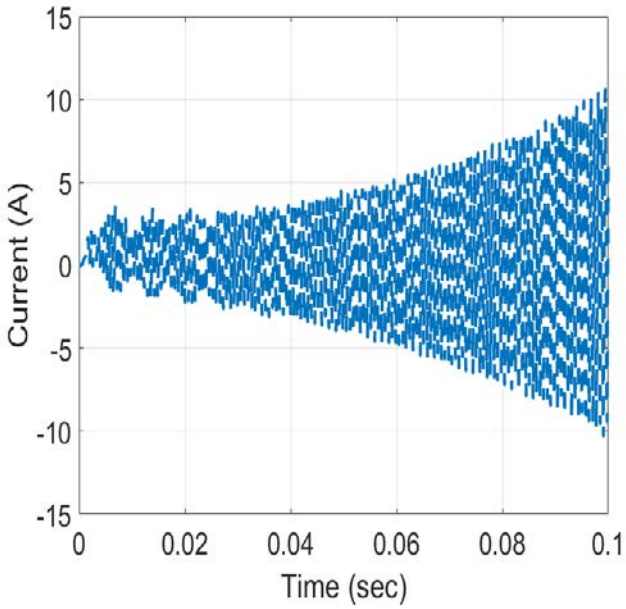

Fig. 12 Current voltage with week anti-saturating action

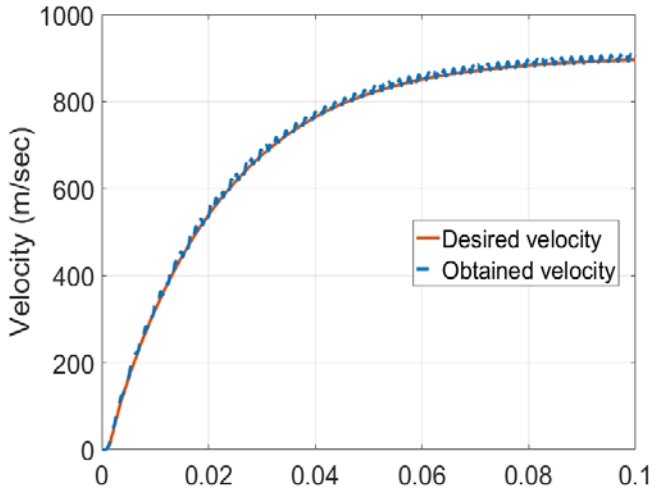

Fig. 13 Velocity tracking in case of adequate values of the elements of matrix **Q**

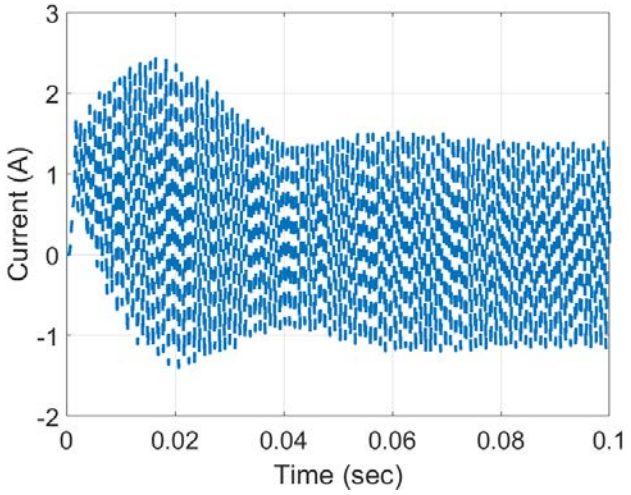

Fig. 14 Current in case of adequate values of the elements of matrix **Q**

4 Conclusion

One of the most important problems in the context of optimization using LMPC is represented by conservative conditions on the stability. This paper presents a sufficient and constructive condition for the stability of a LMPC for one step prediction horizon calculating lower bound of the unique element of matrix **R** which represents the weight of the input in a typical given cost function. A physical interpretation of the result is given in the light of some physical considerations. In the second part of the paper the saturation case is considered and a sufficient condition to obtain stability and saturation avoidance is proven. Two illustrative examples are provided.

References:

[1] P. Mercorelli, A switching Kalman Filter for sensorless control of a hybrid hydraulic piezo actuator using MPC for camless internal combustion engines, In Proceedings of the IEEE International Conference on Control Applications, 2012, pp. 980-985.

[2] P. Mercorelli, A switching model predictive control for overcoming a hysteresis effect in a hybrid actuator for camless internal combustion engines, In Proceedings of the IEEE PRECEDE 2011 – International Workshop on Predictive Control of Electrical drives and Power Electronics, 2011, pp. 10-16.

[3] S.J.Qin and T.A. Badgwell, A survey of industrial model predictive control technology, Control Engineering Practice, Vol.11, No.7 2003, pp.733-764.

[4] S. Bolognani, L. Peretti, and M. Zigliotto, Design and implementation of model predictive control for electrical motor drives, IEEE Transactions on Ind. ustrial Electronics, Vol. 56, No.6, 2009, pp. 1925-1936.

[5] V.A. Neelakantan, G.N. Washington, and N.K. Bucknor, Model predictive control of a two-stage actuation system using piezoelectric actuators for controllable industrial and automotive brakes and clutches, Journal of Intelligent Materials Systems and Structures, Vol.19, No.7, 2008, pp. 845-857.

[6] Z. Hu and D.F. Farson, Design of a waveform tracking system for a piezoelectric actuator, In Proceedings of the Institution of Mechanical Engineers, Vol. 222, 2008, pp. 11-21.

[7] H. Sunan, T.K. Kiong, and L.T. Heng, Applied Predictive Control, Springer-Verlag London, printed in Great Britain, 2002.